**Classification**

Biological Sciences: Biochemistry

**Title**

Conformational activation of ADAMTS13

**Short title for RSS feed**

Conformational activation of ADAMTS13

**Author affiliation**

Kieron South[a], Brenda M Luken[a], James TB Crawley[a] , Rebecca Phillips[a], Mari Thomas[a], Richard F Collins[b], Louis Deforche[c], Karen Vanhoorelbeke[c] and David A Lane[a]

[a]Centre for Haematology, Imperial College London, London, W12 ONN [b]Electron Microscopy Facility, Faculty of Life Sciences, University of Manchester, Manchester, M13 9PL [c] Laboratory for Thrombosis Research, IRF Life Sciences, KU Leuven, Kulak, Kortrijk, Belgium

**Corresponding author**

Kieron South or David A Lane, Commonwealth Building 5S5, Imperial College London, Hammersmith Hospital, Du Cane Road, London, W12 0NN, ksouth@imperial.ac.uk/ 02083832298, or d.lane@imperial.ac.uk/02083832295

**Keywords**

ADAMTS13, Von Willebrand factor, thrombotic thrombocytopenic purpura, haemostasis

**Author contributions**

K.S., J.C., B.L. and D.L. designed research.

K.S., R.C. and R.P. performed research.

K.V., L.D. and M.T. contributed new reagents/analytical tools

K.S., D.L., R.C. and R.P. analysed data.

K.S., R.C. and D.L. interpreted data and generated figures.

K.S. and D.L. wrote the paper.

The authors declare no conflict of interest.

**Abstract**

ADAMTS13 is a metalloprotease that regulates von Willebrand factor (VWF) function. ADAMTS13-mediated proteolysis is determined by conformational changes in VWF but may also depend upon its own conformational activation. Kinetic analysis of WT ADAMTS13 revealed ~2.5 fold reduced activity when compared to ADAMTS13 lacking its C-terminal tail (MDTCS) or its CUB1-2 domains (WTΔCUB1-2), suggesting that the CUB domains naturally limit ADAMTS13 function. Consistent with this, WT ADAMTS13 activity was enhanced ~2.5-fold by preincubation with either an anti-CUB mAb (20E9), or with VWF D4CK (the natural binding partner for the CUB domains). Furthermore, the isolated CUB1-2 domains not only bound MDTCS, but also inhibited activity up to 2.5-fold. Interestingly, a Gain of Function (GoF) ADAMTS13 spacer domain variant (R568K/F592Y/R660K/Y661F/Y665F) was ~2.5-fold more active than WT ADAMTS13, but could not be further activated by 20E9 mAb or VWF D4CK, and was unable to bind or be inhibited by the CUB1-2 domains, suggesting that the inhibitory effects of the CUB domains involve an interaction with the spacer domain that is disrupted in GoF ADAMTS13. Electron microscopy demonstrated a "closed" conformation of WT ADAMTS13, and suggested a more "open" conformation for GoF ADAMTS13. The cryptic spacer domain epitope that is revealed by conformational unfolding also represents the core antigenic target for auto antibodies in TTP. We propose that ADAMTS13 circulates in a "closed" conformation, which is maintained by a CUB-spacer domain binding interaction. ADAMTS13 becomes conformationally activated upon demand through interaction of its C-terminal CUB domains with VWF, making it susceptible to immune recognition.

**Significance statement**

We show a CUB-spacer domain interaction impedes the exposure of the ADAMTS13 spacer functional exosite. This prevents ADAMTS13 from interacting effectively with its complementary binding site in the VWF A2 domain. This CUB-spacer interaction is disrupted by interaction with the C-terminal domains of VWF, leading to conformational activation of ADAMTS13. This study also suggests that activation of ADAMTS13 reveals a cryptic epitope in the spacer domain that constitutes the auto antigenic core in patients with acquired TTP. These antibodies inhibit ADAMTS13, causing deposition of VWF and platelet rich microthrombi in small blood vessels, resulting in organ damage. This study therefore offers an insight into the complexity of both normal haemostatic control and the pathogenesis of auto immunity.

**Introduction**

Von Willebrand factor (VWF) is a large, multidomain glycoprotein that is able to recognise vascular damage by binding to exposed collagen through its A3 domain (1-3). VWF tethered to collagen responds to shear forces by adapting its conformation (4). Under conditions of low shear, it is thought to adopt a globular conformation. At high shear, it unfolds and reveals its binding site for the platelet GpIbα receptor on its A1 domain, thereby facilitating platelet recruitment to the site of vascular injury. A decisive factor in the ability of VWF to capture platelets is its unfolding in response to shear (5).

VWF is heterogeneous with respect to its molecular size due to the varying degrees of multimerisation that occur within the endothelial cell. It is stored, prior to release into the plasma, as multimers that can be as large as 20-40-mers (6-9). Upon release from the cell, it is the highest molecular weight multimers which are haemostatically most active. Indeed, "ultra large" multimers present a potential hazard if their function is unregulated, as they can predispose to the formation of VWF-platelet microthrombi that can occlude small blood vessels, resulting in thrombotic thrombocytopenic purpura (TTP) (10).

The metalloprotease ADAMTS13 is able to cleave the VWF A2 domain and, in doing so, dramatically reduces the multimeric size of VWF and its propensity to form platelet containing microthrombi (11, 12). Cleavage of VWF by ADAMTS13 is a multistep process. An initial interaction takes place between the D4CK domains of globular VWF and ADAMTS13, which may serve to position protease in readiness for the VWF to unfold (13, 14). As unfolding occurs, exposure of the scissile bond, Y1605-M1606, of the A2 domain is controlled by structural elements contained within this domain (15-18). Progressive unfolding allows distinct functional exosites within its A2 domain to be exposed and engaged by complementary binding sites on the protease, spacer and disintegrin-like domains (19-23). Ultimately, docking of VWF scissile bond P1', P1 and P3 residues into sub-sites on the protease, position the scissile bond for cleavage (24). Conformational changes in VWF are therefore essential for its efficient cleavage by ADAMTS13.

In order to explore the possible role of conformation in ADAMTS13 function (25, 26), we have studied a recently described gain of function variant of ADAMTS13 (27). Jian *et al*. concluded that an ADAMTS13 variant comprising composite spacer domain substitutions R568K/F592Y/R660K/Y661F/Y665F (in what follows to be designated "GoF") had ~4-fold increased ability to cleave VWF substrates (27). A similar increase in activity has also been observed previously by others upon removal of the C-terminal domains from ADAMTS13 (28). Based upon our investigation of the properties of ADAMTS13, the GoF variant and their derivatives, reported herein, we propose that ADAMTS13 adopts a globular conformation determined by interaction of its spacer and CUB domains.

## Results

### Increased substrate recognition leads to hyperactivity in GoF ADAMTS13

We have conducted a kinetic analysis of VWF115 cleavage and propose that there is a ~2 fold difference between WT ADAMTS13 and the GoF variant (27) (Figure 1A and $k_{cat}/K_m$ values in Table 1). There was, however, no difference in $k_{cat}$ and the enhanced activity is instead due to an increased affinity for the substrate, as demonstrated by the $K_m$ values of 1.54 µM and 0.86 µM for WT and GoF ADAMTS13, respectively ($p < 0.05$). The $K_{D(APP)}$ values determined by equilibrium plate binding assays suggested a 2-fold increased affinity of GoF ADAMTS13 for VWF (Figure 1B). This was confirmed by both steady state and global fit SPR analysis (Figure 1C, 1D and 1E) and was shown to be caused by an increased rate of association (Table 1, $p < 0.001$).

### Disruption of C-terminal interactions activates WT ADAMTS13

The first step in VWF recognition by ADAMTS13 is mediated by binding of the VWF D4CK domains of globular VWF to the C-terminal domains of ADAMTS13 (13, 14). We hypothesised that this initial binding causes a conformational activation of ADAMTS13 that may be unnecessary in the GoF variant. Addition of the VWF D4CK domain fragment to WT ADAMTS13 in a FRETS-VWF73 assay increased its activity (normalised against that of WT ADAMTS13) in a dose dependent manner, resulting in a 2-2.5 fold increase (Figure 2A and 2C, $p < 0.001$). This hyperactivity was similar to that exhibited by GoF ADAMTS13. Furthermore the activity of GoF ADAMTS13 was not then enhanced by VWF D4CK addition (Figure 2B and 2C).

The 20E9 mAb recognises the CUB2 domain of ADAMTS13. Enhanced activity was observed upon addition of the 20E9 mAb to WT ADAMTS13 (Figure 2D and 2F, $p < 0.001$), reaching a maximal enhanced activity of 2.5 fold. GoF ADAMTS13 was unaffected by the antibody (Figure 2E and 2F), suggesting that the CUB domains may play an important role in ADAMTS13 activation.

### Regulation of ADAMTS13 activity by the CUB domains

We hypothesised that the C-terminal CUB domains interact with the spacer domain in the native WT ADAMTS13. We predicted that removal of the C-terminal domains (in the truncated variant MDTCS) would produce a similar activity enhancement to that observed with VWF D4CK and with 20E9 mAb. Indeed, both WT and GoF MDTCS variants are fully hyperactive with activity profiles indistinguishable from GoF ADAMTS13 (Figure 3A, 3B and 3C).

Moreover, truncation of ADAMTS13 after the TSP2-8 domains (WTΔCUB1-2 variant) produced an enhancement similar to that observed in WT MDTCS (Figure 3D and 3F). Furthermore, reintroduction of the isolated CUB1-2 domain fragment had a dose-dependent inhibitory effect on both WT MDTCS and WTΔCUB1-2, reducing activity similar to that of WT ADAMTS13 (Figure 3A and 3D). In contrast, C-terminal truncation of GoF ADAMTS13 had no influence on its activity and addition of the CUB1-2 domain fragment was ineffective even at high concentrations (Figures 3B and 3E).

**A CUB-spacer domain binding interaction**

We developed a reciprocal co-immunoprecipitation (co-IP) experiment to directly analyse any CUB-spacer domain interaction. WT MDTCS and the CUB1-2 domain fragment bound in solution and remained in complex when either fragment was pulled down specifically by mAb. This resulted in both fragments being detected in immunoprecipitation (IP) eluates and depleted from solution (Figure 4A). In contrast, when GoF MDTCS and CUB1-2 were incubated, only the fragment being pulled down by its corresponding mAb was detected in the eluate, with the other fragment remaining in solution. As GoF MDTCS differs from WT MDTCS only by its spacer domain substitutions, this strongly suggested that the spacer domain is the site of CUB domain binding to MDTCS.

We further refined this approach to allow the quantification of binding and elution of MDTCS from CUB1-2 immobilised on magnetic beads (see 'Experimental Procedures'). This allowed us to perform MDTCS-CUB co-IP over a range of MDTCS concentrations and to accurately quantify bound and free MDTCS. A $K_{D(APP)}$ value of ~40 nM was determined for the binding of CUB1-2 and WT MDTCS (Figure 4B). In agreement with earlier co-IP experiments, minimal binding was observed between CUB1-2 and GoF MDTCS.

**ADAMTS13 can exist in a 'closed' or more 'open' conformation**

Binding of the CUB domains to the spacer domain in WT ADAMTS13 would require flexibility in the C-terminal domains. We hypothesised that this would result in an observable change in the overall conformation of the full length protein and we observed this using TEM of negatively stained proteins (Figure 5). Analysis of the WT ADAMTS13 sample produced a variety of different monodisperse orientational particles measuring between 12-16nm, consistent with a protein ~170 kDa in size. The main projection view had a clear compact, globular conformation with an additional side 'bulge' of projection density (Figure 5A – panel 3); we have assigned this as the 'closed' ADAMTS13 conformation, which corresponds to the native ADAMTS13. Examination of a similar number of GoF ADAMTS13 particles, revealed similar sized particles, but the projection averages produced were somewhat more linear (Figure 5B – panel 3) and the projection view with the side 'bulge' was absent. The projections were also not as sharply delineated as the ADAMTS13 samples and this combined with a different population of particle projections suggests that the complex has adopted a more open organisation with some local region of protein in a flexible/unstructured conformation (Figure 5 – end panel). These results are compatible with exposure of spacer domain VWF binding exosites and hyperactivity.

**WT ADAMTS13 conformational activation reveals its cryptic TTP auto antibody binding epitopes**

WT ADAMTS13 was inhibited by TTP patient auto antibodies and the single TTP patient derived II-1 mAb (29) in FRETS-VWF73 assays (Figure 6A). However, despite there being a large excess of these antibodies added to activity assays, ADAMTS13 was only inhibited by 60%, compared to 95% inhibition of MDTCS by the same TTP aAb (Figure 6C). This suggests that WT ADAMTS13, in its 'closed' and relatively inactive state, might not be readily recognised by these antibodies. This was

confirmed by IP of WT ADAMTS13 by the II-1 mAb covalently linked to magnetic beads. When converted to its 'open' conformation using the activating 20E9 mAb (Figure 6D), or VWF D4CK fragment (Figure 6E), recognition of WT ADAMTS13 was dramatically increased. The spacer domain mutations in GoF ADAMTS13 have been shown previously to abolish this antigenicity (see also Figure 6B); this was confirmed in this study in both FRET and IP assays (Figure 6D and Figure 6E).

**Discussion**

The concept of conformational activation of ADAMTS13 has been alluded to previously as a possible explanation for suggested conflicting roles of the CUB domains (25, 30). We present here results which indicate that ADAMTS13 naturally adopts a folded or closed conformation, with folding mediated through an interaction between the C-terminal CUB domains and the more central spacer domain. The importance of this folding is suggested by the known functional importance of the spacer domain, which serves as a critical exosite that interacts with a cryptic binding site revealed on the VWF A2 domain as it unfolds (31). This provides an essential localising mechanism that helps position the ADAMTS13 protease domain within reach of the VWF scissile bond. A consequence of the folded conformation of ADAMTS13 is that the important spacer domain exosite is only partially available and requires full exposure to enable proteolysis of VWF to proceed efficiently. It is now established that ADAMTS13 can interact with globular VWF through recognition of its surface exposed C-terminal domains, D4CK, by the TSP-CUB domain region of ADAMTS13 (13, 14). This binding interaction has been regarded as a positioning one, enabling a small amount of ADAMTS13 to associate reversibly with VWF in its globular conformation, pending VWF unfolding (14). However, we now present evidence that the VWF D4CK fragment can increase the activity of ADAMTS13 in a FRETS-VWF73 assay. We suggest, therefore, that on binding to the VWF D4CK domains, ADAMTS13 unfolds, to fully expose its cryptic spacer domain exosite. Once unfolded, the spacer domain can directly contact its VWF A2 complementary interaction site and enhance the cleavage process. The precise mechanism for VWF D4CK activation requires further investigation, but it is plausible to suggest that its binding to the region around or including the CUB domains disrupts the spacer-CUB binding interaction, causing unfolding and activation.

An interaction between the spacer and CUB domains of ADAMTS13 is supported by the results of addition of activating mAb, as well as activity and binding assays of C-terminal truncated WT ADAMTS13 in the presence of isolated CUB fragments. Concerning the activating mAb, we have shown that 20E9 mAb, an antibody that recognises the CUB2 domain region of ADAMTS13, can increase the activity of WT ADAMTS13. In FRETS-VWF73 assays, isolated CUB fragments inhibit the proteolytic activities of both WT MDTCS and WTΔCUB1-2 truncation variants. Furthermore, in solution binding pull down experiments, we have shown that CUB fragments can directly bind to these derivatives, with an estimated affinity of ~40 nM. Although these experiments necessarily used free CUB domain fragments, which might not interact with the spacer domain in exactly the same way or with the same affinity when contiguous with their neighbouring TSP domains, they do provide compelling evidence of a moderate affinity binding interaction between spacer and CUB domains. Furthermore, the isolated CUB domain fragments inhibited WTΔCUB1-2, which retains its TSP domains, suggesting that the CUB binding site on the spacer domain was not introduced by complete deletion of these C-terminal domains.

Additional evidence for conformational activation of ADAMTS13 comes from our characterisation of GoF ADAMTS13. This variant is shown to have an enhanced association rate with VWF fragments leading to ~2-2.5 fold overall enhanced cleavage of the scissile bond. The properties of this variant might arise in part because of an increased molecular recognition of its substrate induced by the 5 introduced substitution mutations in the spacer domain. Alternatively, the enhanced activities could also arise by disruption of the spacer-CUB domain interaction in this variant by the introduced spacer domain substitution mutations. We propose that this variant adopts a native unfolded conformation and is therefore essentially preactivated. Support for this idea is provided by its enhanced association rate with VWF115 and by failure of 20E9 activating antibodies to enhance activity of the variant. It is again interesting that pull down experiments with GoF MDTCS could not show it binding the isolated CUB1-2 domain fragment. Moreover, the lack of inhibition in FRETS-VWF73 assay by the CUB domain fragment of GoF MDTCS and GoFΔCUB1-2 truncation variants provides further support for lack of a masking interaction by the CUB domains and therefore a preactivation state. From our TEM experiments we have visualised WT ADAMTS13 as a globular molecule while GoF ADAMTS13 appears to be less compact.

A potential advantage of conformational activation of ADAMTS13 is that localisation of the activated form of the protease will occur on the surface of its substrate, VWF. It is conceivable that this might offer a protective mechanism, particularly as it has been demonstrated that ADAMTS13 is susceptible to cleavage by several coagulation proteases (32, 33). But conformational activation can also have untoward consequences. It has been recognised that auto antibodies against ADAMTS13 cause or predispose to acquired TTP (34). The trigger factors that initiate the auto immune response have yet to be fully delineated. It is interesting that the majority of patients with TTP have auto antibodies that are directed to the ADAMTS13 spacer domain (20, 35, 36). We propose that this is because this domain is naturally cryptic, shielded by the CUB domains. During the process of ADAMTS13 activation the cryptic epitope(s) are revealed and might be recognised as foreign during a concurrent immune activation. Support for this concept is provided by the increased recognition of WT ADAMTS13 spacer domain by the patient derived II-1 mAb when the activating 20E9 antibody or VWF D4CK fragment is present. Consequently, our results on the conformational activation of ADAMTS13 provide insight to both the proteolytic process by which ADAMTS13 recognises VWF and to the mechanism of auto antibody formation in TTP.

## Experimental Procedures

### Production of recombinant ADAMTS13 and VWF fragments

Recombinant human ADAMTS13 with a C-terminal Myc/$His_6$ tag in pCDNA3.1 (32) was used to generate GoF ADAMTS13 (R568K/F592Y/R660K/Y661F/Y665F) by sequential site directed mutagenesis. The same mutagenesis primers were also used to introduce the GoF mutations into WT MDTCS-Myc/ $His_6$. The truncated variants WTΔCUB1-2 and GoFΔCUB1-2 and the CUB1-2 domain fragment were generated by inverse PCR using the full length ADAMTS13 constructs. All ADAMTS13 variants and fragments were expressed in HEK293S cells, purified and quantified using in house ELISAs as described previously (37). For electron microscopy, ADAMTS13 was purified to homogeneity by gel filtration using a Superose 12 10/300 GL column (GE Healthcare).

The VWF A2 domain fragment VWF115 (VWF residues 1554-1668) was expressed and purified as previously described (32). The VWF D4CK domain fragment (VWF residues 1874-2813) in the vector pcDNA 3.1/His was transiently expressed in HEK293S, purified by FPLC and quantified by ELISA (13).

**Production and characterization of anti-ADAMTS13 mAb 20E9**

The 20E9 mAb was one of 30 anti-ADAMTS13 mAbs obtained after immunisation of WT Balb/c mice with recombinant WT ADAMTS13, followed by fusion of their spleen cells with Sp2/0 myeloma cells. The epitope of mAb 20E9 is situated in the CUB2 domain as determined through epitope mapping using a series of ADAMTS13 variants where all domains were individually deleted.

**TTP patient IgG preparation**

Total IgG was isolated from the presentation plasma sample of a TTP patient with high titre anti-ADAMTS13 IgG directed against the spacer domain, using melon gel spin columns (Thermo Scientific). Ethical approval for the use of the sample was previously obtained from the local Research Ethics Committee (reference:08/H0716/72).

**ADAMTS13 activity assays**

Recombinant VWF A2 domain fragments VWF115 (VWF residues 1554-1668) and FRETS-VWF73 (VWF residues 1596-1668) which span the ADAMTS13 cleavage site and spacer domain binding exosites, were used as proteolytic substrates to determine the activity of ADAMTS13 and its variants. Cleavage of VWF115 by ADAMTS13 was carried out as described (19). For FRETS-VWF73 assays ADAMTS13, MDTCS and ΔCUB1-2 variants (WT and GoF) were diluted to 0.3 nM in reaction buffer (5 mM Bis-Tris, pH 6.0/25 mM $CaCl_2$/0.005% Tween-20) in white 96-well plates (Nunc). Purified CUB1-2 domain fragment, VWF D4CK, 20E9 mAb, II-1 mAb or TTP patient IgG were added before being pre-incubated for 45 min at 37 °C. The reaction was initiated by the addition of an equal volume of 4 µM FRETS-VWF73 substrate (Peptanova GMBH). Fluorescence (excitation 340 nm; emission 460 nm) was measured at 30°C at 1 minute intervals for 1 hour using a Fluostar Omega plate reader (BMG Labtech). Results were normalised to WT ADAMTS13 activity to allow cross comparison of any changes.

**Equilibrium plate binding assay and surface plasmon resonance**

Binding of VWF115 to ADAMTS13 was determined by equilibrium plate binding assay (13, 19), and by surface plasmon resonance using a BIAcore T100 system (BIAcore) as described (13).

**Co-immunoprecipitation analysis of CUB and MDTCS interaction**

Samples containing 40 nM MDTCS (WT or GoF), in the absence/presence of 40 nM CUB1-2 fragment, were immunoprecipitated using Protein G Dynabeads (Invitrogen) coupled to either the 3H9 mAb against the ADAMTS13 metalloprotease domain (33, 38), the 20E9 mAb directed against the ADAMTS13 CUB domains or the IgG isotype control 15D7 mAb (39). Beads were washed, and bound

protein eluted in 1x LDS loading buffer at 70 °C for 10 min. Inputs (pre-IP), flow through (post-IP) and bound protein in eluates were analysed by SDS PAGE and anti-ADAMTS13 western blot.

For CUB-MDTCS affinity determination, blocked and 20E9 mAb coated Dynabeads were pre-incubated with 100 nM CUB1-2 domain fragment and used to immunoprecipitate MDTCS (WT or GoF) at increasing concentrations (5-200 nM). Bound MDTCS was eluted in 20 mM Tris, pH 7.4/1 M NaCl. Bound and free MDTCS concentrations were determined by in house ELISA and $K_D$ values were determined by fitting data to a one site binding hyperbola using Prism 4 software (Graphpad).

**TTP auto antibody binding**

The TTP patient derived II-1 mAb (29) (kindly provided by Prof J. Voorberg and Dr N. Sorvillo) was covalently coupled to M280 tosylactivated Dynabeads (Invitrogen) following manufacturer's instructions. The coupled beads were added to 40 nM ADAMTS13 (WT or GoF) and pre-incubated for 1 hour at 37 °C in the absence/presence of 4 µg 20E9 mAb. After 4 hours incubation, the beads were washed and bound protein eluted in LDS loading buffer. Inputs (pre-IP), flow through (post-IP) and eluates were analysed by SDS PAGE and anti-ADAMTS13 western blot.

**Transmission electron microscopy**

Fully purified samples of ADAMTS13 variants (10 µl of ~10 µg/ml) in 20 mM Tris pH 7.8/150 mM NaCl/5 mM $CaCl_2$ were applied to glow-discharged continuous carbon-coated 400-mesh copper grids (TAAB Laboratories) for 1 minute. Excess sample was blotted using Whatman paper and the protein was negatively stained by the addition of 10 µl 5 % (w/v) uranyl acetate for 1 minute. Images were acquired at a nominal magnification of 39,000x using a Philips Tecnai30 Polara FEG electron microscope operating at 200 kV low-dose mode and recorded on a Gatan 4K charge-coupled device camera.

Image analysis of the recorded TEM DM3 data files was performed using EMAN2 (http://blake.bcm.edu/emanwiki/EMAN2). Equivalent datasets of ~6000 particles were boxed out of images using semi-automated swarm picking; any aggregated or overlapping data were discarded. Data were CTF corrected and the dataset underwent multi-statistical reference-free 2-D classification. Data were auto-masked, a maximum shift of 5 pixels was applied and cross correlation coefficient (CCC) was used as the main comparator. Projection averages of each particle orientations were selected and a low pass Gaussian filter (20 Angstroms) was applied.

**Acknowledgements**

This work was funded by a grant from the British Heart Foundation (PG/12/55/29740) awarded to D.L., J.C. and B.L., by grant G.0584.11 from the 'Fonds voor Wetenschappelijk Onderzoek (FWO)' Flanders Belgium awarded to K.V. and by a Ph.D. grant of the Agency for Innovation by Science and Technology (IWT), awarded to L.D. We are grateful to Professor Jan Voorberg and Dr Nicoletta Sorvillo, Sanquin-AMC Landsteiner Laboratory, for providing the II-1 mAb and to Dr Marie Scully, University College London, for providing the TTP patient plasma sample.

**References**


1. Sadler JE (1998) Biochemistry and genetics of von Willebrand factor. *Annual review of biochemistry* 67:395-424.
2. Mohri H, Yoshioka A, Zimmerman TS, & Ruggeri ZM (1989) Isolation of the von Willebrand factor domain interacting with platelet glycoprotein Ib, heparin, and collagen and characterization of its three distinct functional sites. *The Journal of biological chemistry* 264(29):17361-17367.
3. Roth GJ, Titani K, Hoyer LW, & Hickey MJ (1986) Localization of binding sites within human von Willebrand factor for monomeric type III collagen. *Biochemistry* 25(26):8357-8361.
4. Siedlecki CA*, et al.* (1996) Shear-dependent changes in the three-dimensional structure of human von Willebrand factor. *Blood* 88(8):2939-2950.
5. Zhang Q*, et al.* (2009) Structural specializations of A2, a force-sensing domain in the ultralarge vascular protein von Willebrand factor. *Proceedings of the National Academy of Sciences of the United States of America* 106(23):9226-9231.
6. Mayadas TN & Wagner DD (1992) Vicinal cysteines in the prosequence play a role in von Willebrand factor multimer assembly. *Proceedings of the National Academy of Sciences of the United States of America* 89(8):3531-3535.
7. Wise RJ, Pittman DD, Handin RI, Kaufman RJ, & Orkin SH (1988) The propeptide of von Willebrand factor independently mediates the assembly of von Willebrand multimers. *Cell* 52(2):229-236.
8. Schneider SW*, et al.* (2007) Shear-induced unfolding triggers adhesion of von Willebrand factor fibers. *Proceedings of the National Academy of Sciences of the United States of America* 104(19):7899-7903.
9. Hoyer LW & Shainoff JR (1980) Factor VIII-related protein circulates in normal human plasma as high molecular weight multimers. *Blood* 55(6):1056-1059.
10. Moake JL*, et al.* (1982) Unusually large plasma factor VIII:von Willebrand factor multimers in chronic relapsing thrombotic thrombocytopenic purpura. *The New England journal of medicine* 307(23):1432-1435.
11. Tsai HM (1996) Physiologic cleavage of von Willebrand factor by a plasma protease is dependent on its conformation and requires calcium ion. *Blood* 87(10):4235-4244.
12. Furlan M, Robles R, & Lammle B (1996) Partial purification and characterization of a protease from human plasma cleaving von Willebrand factor to fragments produced by in vivo proteolysis. *Blood* 87(10):4223-4234.
13. Zanardelli S*, et al.* (2009) A novel binding site for ADAMTS13 constitutively exposed on the surface of globular VWF. *Blood* 114(13):2819-2828.
14. Feys HB, Anderson PJ, Vanhoorelbeke K, Majerus EM, & Sadler JE (2009) Multi-step binding of ADAMTS-13 to von Willebrand factor. *Journal of thrombosis and haemostasis : JTH* 7(12):2088-2095.
15. Lynch CJ, Lane DA, & Luken BM (2014) Control of VWF A2 domain stability and ADAMTS13 access to the scissile bond of full-length VWF. *Blood* 123(16):2585-2592.
16. Marti T, Rosselet SJ, Titani K, & Walsh KA (1987) Identification of disulfide-bridged substructures within human von Willebrand factor. *Biochemistry* 26(25):8099-8109.

17. Zhou M*, et al.* (2011) A novel calcium-binding site of von Willebrand factor A2 domain regulates its cleavage by ADAMTS13. *Blood* 117(17):4623-4631.
18. Luken BM, Winn LY, Emsley J, Lane DA, & Crawley JT (2010) The importance of vicinal cysteines, C1669 and C1670, for von Willebrand factor A2 domain function. *Blood* 115(23):4910-4913.
19. Zanardelli S*, et al.* (2006) ADAMTS13 substrate recognition of von Willebrand factor A2 domain. *The Journal of biological chemistry* 281(3):1555-1563.
20. Pos W*, et al.* (2010) An autoantibody epitope comprising residues R660, Y661, and Y665 in the ADAMTS13 spacer domain identifies a binding site for the A2 domain of VWF. *Blood* 115(8):1640-1649.
21. de Groot R, Bardhan A, Ramroop N, Lane DA, & Crawley JT (2009) Essential role of the disintegrin-like domain in ADAMTS13 function. *Blood* 113(22):5609-5616.
22. de Groot R, Lane DA, & Crawley JT (2010) The ADAMTS13 metalloprotease domain: roles of subsites in enzyme activity and specificity. *Blood* 116(16):3064-3072.
23. Crawley JT, de Groot R, Xiang Y, Luken BM, & Lane DA (2011) Unraveling the scissile bond: how ADAMTS13 recognizes and cleaves von Willebrand factor. *Blood* 118(12):3212-3221.
24. Xiang Y, de Groot R, Crawley JT, & Lane DA (2011) Mechanism of von Willebrand factor scissile bond cleavage by a disintegrin and metalloproteinase with a thrombospondin type 1 motif, member 13 (ADAMTS13). *Proceedings of the National Academy of Sciences of the United States of America* 108(28):11602-11607.
25. Tao Z*, et al.* (2005) Recombinant CUB-1 domain polypeptide inhibits the cleavage of ULVWF strings by ADAMTS13 under flow conditions. *Blood* 106(13):4139-4145.
26. Muia J, *et al*. (2014) Abstracts of the 60th annual meeting of the scientific and standardization committee of the international society on thrombosis and haemostasis june 23-26, 2014. *Journal of thrombosis and haemostasis : JTH* 12 Suppl 1:1-106.
27. Jian C*, et al.* (2012) Gain-of-function ADAMTS13 variants that are resistant to autoantibodies against ADAMTS13 in patients with acquired thrombotic thrombocytopenic purpura. *Blood* 119(16):3836-3843.
28. Gao W, Anderson PJ, Majerus EM, Tuley EA, & Sadler JE (2006) Exosite interactions contribute to tension-induced cleavage of von Willebrand factor by the antithrombotic ADAMTS13 metalloprotease. *Proceedings of the National Academy of Sciences of the United States of America* 103(50):19099-19104.
29. Pos W*, et al.* (2009) VH1-69 germline encoded antibodies directed towards ADAMTS13 in patients with acquired thrombotic thrombocytopenic purpura. *Journal of thrombosis and haemostasis : JTH* 7(3):421-428.
30. Majerus EM, Anderson PJ, & Sadler JE (2005) Binding of ADAMTS13 to von Willebrand factor. *The Journal of biological chemistry* 280(23):21773-21778.
31. Gao W, Anderson PJ, & Sadler JE (2008) Extensive contacts between ADAMTS13 exosites and von Willebrand factor domain A2 contribute to substrate specificity. *Blood* 112(5):1713-1719.
32. Crawley JT*, et al.* (2005) Proteolytic inactivation of ADAMTS13 by thrombin and plasmin. *Blood* 105(3):1085-1093.
33. Feys HB*, et al.* (2010) Inactivation of ADAMTS13 by plasmin as a potential cause of thrombotic thrombocytopenic purpura. *Journal of thrombosis and haemostasis : JTH* 8(9):2053-2062.

34. Furlan M*, et al.* (1998) von Willebrand factor-cleaving protease in thrombotic thrombocytopenic purpura and the hemolytic-uremic syndrome. *The New England journal of medicine* 339(22):1578-1584.
35. Luken BM*, et al.* (2005) The spacer domain of ADAMTS13 contains a major binding site for antibodies in patients with thrombotic thrombocytopenic purpura. *Thrombosis and haemostasis* 93(2):267-274.
36. Klaus C*, et al.* (2004) Epitope mapping of ADAMTS13 autoantibodies in acquired thrombotic thrombocytopenic purpura. *Blood* 103(12):4514-4519.
37. Chion CK, Doggen CJ, Crawley JT, Lane DA, & Rosendaal FR (2007) ADAMTS13 and von Willebrand factor and the risk of myocardial infarction in men. *Blood* 109(5):1998-2000.
38. Feys HB*, et al.* (2010) Thrombotic thrombocytopenic purpura directly linked with ADAMTS13 inhibition in the baboon (Papio ursinus). *Blood* 116(12):2005-2010.
39. Schoolmeester A*, et al.* (2004) Monoclonal antibody IAC-1 is specific for activated alpha2beta1 and binds to amino acids 199 to 201 of the integrin alpha2 I-domain. *Blood* 104(2):390-396.

**Figure legends**

**Figure 1. The increased VWF115 binding affinity and proteolytic activity of GoF ADAMTS13. A**, ADAMTS13 variants were incubated with increasing concentrations of VWF115 and initial rates of substrate proteolysis were used to determine $k_{cat}$ and $K_m$ values (listed in Table 1). **B**, the increased substrate recognition suggested by the reduced $K_m$ of the GoF ADAMTS13 variant was confirmed by equilibrium plate binding assay. A 2 fold reduction in $K_{D(APP)}$ was confirmed by SPR using both steady state (**C**) and global fit analysis (**D** and **E**) . The results presented are representative of three independent experiments.

**Figure 2. WT ADAMTS13 activity can be enhanced by the addition of a VWF D4CK domain fragment or by the addition of an activating mAb targeting the CUB2 domain. A-C**, the effect of the VWF D4CK domain fragment on ADAMTS13 activity was determined using the FRETS-VWF73 assay. WT and GoF ADAMTS13 were pre-incubated with varying concentrations of the VWF C-terminal fragment before initiation of the assay by the addition of FRETS-VWF73. GoF ADAMTS13 activity was >2 fold higher than WT ADAMTS13 and was not further increased by VWF D4CK. **D-F**, the effect of the activating mAb was assessed in the same manner. The antibody elicited a >2-fold increase in activity of the WT but had no effect on the already hyperactive GoF variant. Results are presented as mean ± S.E.M. (n=3).

**Figure 3. WT ADAMTS13 hyperactivity resulting from C-terminal truncation can be inhibited by the CUB1-2 domains. A-C**, the activity of WT and GoF MDTCS variants were determined by FRETS-

VWF73 assay. Both enzymes exhibit hyperactivity when compared to WT ADAMTS13. WT MDTCS activity can be inhibited by the addition of CUB1-2 domain fragment, however the fragment has no significant effect on GoF MDTCS. **D-F**, specific removal of the CUB-domains from both WT and GoF ADAMTS13 also results in a >2 fold increase in activity. The CUB1-2 domain fragment displays an inhibitory activity when added to WTΔCUB1-2, albeit at higher concentrations than are required for WT MDTCS inhibition. Results are presented as mean ± S.E.M. (n=3).

**Figure 4. The CUB1-2 domain fragment binds to WT MDTCS through the spacer domain. A**, MDTCS (filled arrowhead) and CUB1-2 (present also as a partially cleaved, faster mobility fragment) (open arrowheads) were immunoprecipitated using Protein G beads coupled to the indicated mAb (3H9, directed to the protease domain, or 20E9, directed to the CUB2 domain). The MDTCS and CUB fragments present in solution pre/post IP, and bound proteins after elution, were detected by polyclonal anti-ADAMTS13 western blot. Co-IP of WT MDTCS with CUB1-2 is evident under both experimental conditions but binding of GoF MDTCS was not apparent. MDTCS and CUB1-2 were also incubated with an isotype control IgG (15D7 mAb). **B**, Affinity between the CUB and spacer domains was determined with WT and GoF MDTCS at a range of concentrations (5-200 nM) and IP using magnetic beads coated with 20E9 mAb complexed to the CUB1-2 domain fragment. Bound and free MDTCS were determined by ELISA and used to derive a $K_D$ of 41.6 ± 3.4 nM for WT MDTCS.

**Figure 5. The proposed alteration of WT ADAMTS13 conformation upon activation.** TEM analysis of WT ADAMTS13 (**A**) and GoF ADAMTS13 (**B**). The figure shows representative examples of negatively stained TEM fields of view, individual particles selected for analysis and the results of multi-statistical reference-free class averaging. Scale bars are all 50nm. The last panel shows a schematic representation of WT ADAMTS13 conformation. This is compatible with the existence of an interaction between the CUB domains (C1 and C2) and spacer domain (S), shielding the VWF A2 domain binding exosites. We propose that activation results in a more linear and flexible 'open' ADAMTS13 conformation which would expose cryptic spacer domain exosites allowing engagement of the unfolded VWF A2 domain.

**Figure 6. WT ADAMTS13 recognition and inhibition by TTP auto antibodies is enhanced upon activation by the anti-CUB 20E9 mAb but is abolished in the GoF variant. A**, proteolysis of the FRETS-VWF73 substrate by WT ADAMTS13 is markedly decreased when the enzyme is pre-incubated with either TTP patient total IgG or TTP patient derived II-1 mAb. **B**, GoF ADAMTS13 activity in FRETS-VWF73 assays is increased 2-fold compared to WT ADAMTS13 (see panel **C**), however it is not impaired by either antibody. Immunoprecipitation of ADAMTS13 in solution using the II-1 mAb covalently coupled to magnetic beads suggests that WT ADAMTS13 is not efficiently recognised. Pre-treatment of WT ADAMTS13 with the activating anti-CUB 20E9 mAb (**D**) or the VWF D4CK domain fragment (**E**) greatly increases its capture by the beads.

**Figure 1**

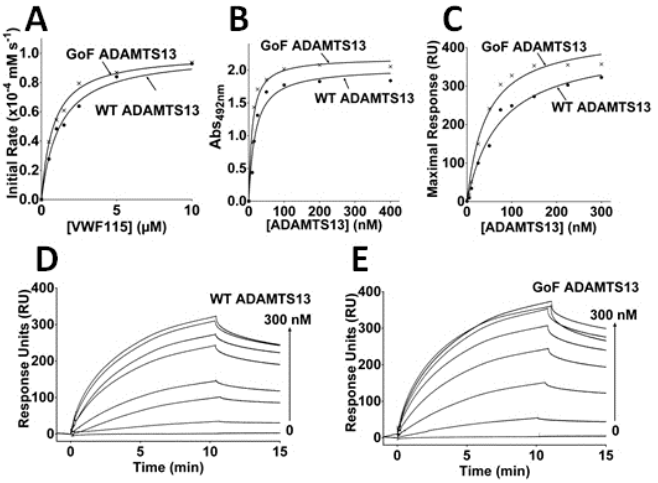


**Table 1**

**Table 1. The activity and VWF115 binding affinity of ADAMTS13 variants**

| | VWF Proteolysis | | | | VWF115 Binding | | | | |
|---|---|---|---|---|---|---|---|---|---|
| | | | | | Plate Binding | SPR Global Fitting | | | SPR $RU_{max}$ |
| | $k_{cat}$ | $K_m$ | $k_{cat}$ / $K_m$ | $k_{cat}$ / $K_m$ (Time course) | $K_{D(APP)}$ | $k_a$ | $k_d$ | $K_D$ | $K_D$ |
| | ($s^{-1}$) | (μM) | ($10^5$ $M^{-1}$ $s^{-1}$) | ($10^5$ $M^{-1}$ $s^{-1}$) | (nM) | ($10^4$ $M^{-1}$ $s^{-1}$) | ($10^{-3}$ $s^{-1}$) | (nM) | (nM) |
| **WT ADAMTS13** | 0.71±0.09 | 1.54±0.20 | 4.1±0.5 | 5.5±0.7 | 26.4±3.0 | 3.72±0.16 | 2.58±0.01 | 72.3±1.3 | 69.8±6.2 |
| **GoF ADAMTS13** | 0.62±0.02 | 0.86±0.07 | 8.3±0.7 | 10.4±0.3 | 11.5±1.4 | 6.82±0.19 | 2.64±0.01 | 38.5±1.2 | 35.8±2.6 |

The activities of ADAMTS13 variants were determined by kinetic analysis of the initial rates of VWF115 proteolysis. The binding interactions between VWF115 and ADAMTS13 variants were determined by equilibrium plate binding assays ($K_{D(APP)}$) and SPR ($k_a$, $k_d$ and $K_D$) Mean values±SEM are based on 3 independent experiments.

**Figure 2**

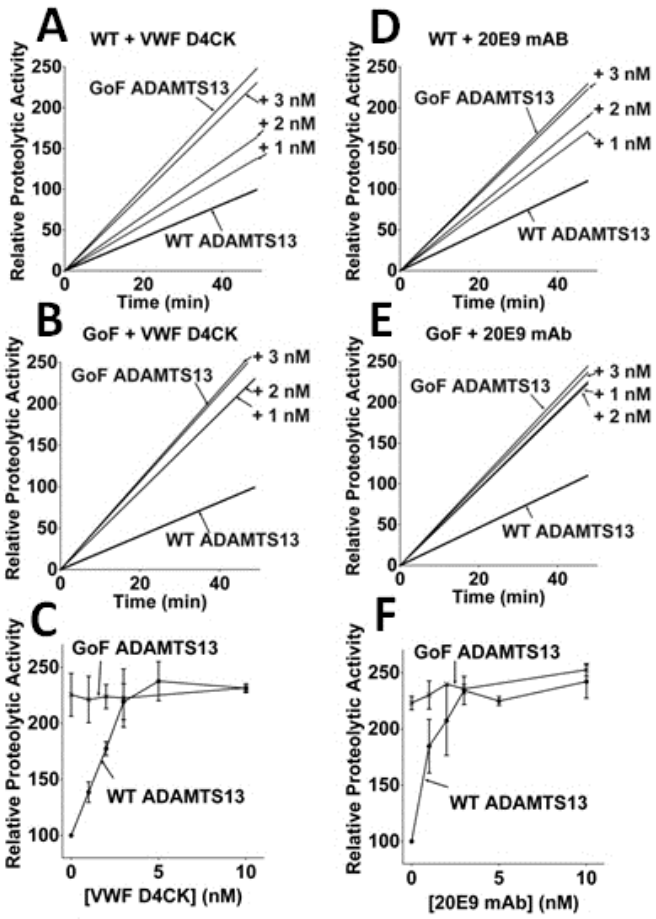
A
WT + VWF D4CK
GoF ADAMTS13
+ 3 nM
+ 2 nM
+ 1 nM
WT ADAMTS13
Relative Proteolytic Activity
Time (min)
B
GoF + VWF D4CK
C
[VWF D4CK] (nM)
D
WT + 20E9 mAB
E
GoF + 20E9 mAb
F
[20E9 mAb] (nM)

**Figure 3**

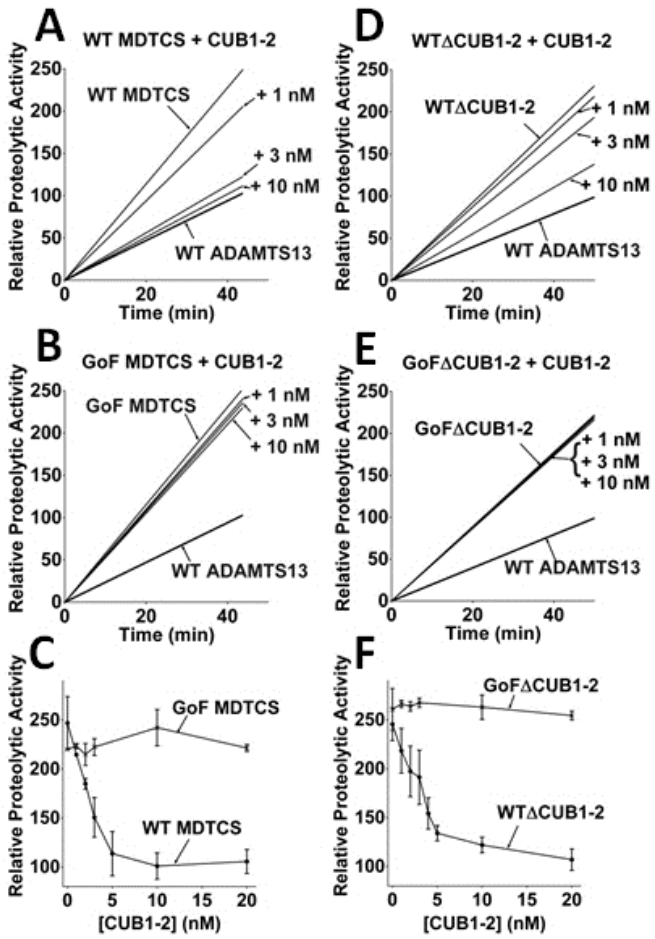
A
WT MDTCS + CUB1-2
WT MDTCS
+ 1 nM
+ 3 nM
+ 10 nM
WT ADAMTS13
Relative Proteolytic Activity
Time (min)
D
WTΔCUB1-2 + CUB1-2
WTΔCUB1-2
+ 1 nM
+ 3 nM
+ 10 nM
WT ADAMTS13
Relative Proteolytic Activity
Time (min)
B
GoF MDTCS + CUB1-2
GoF MDTCS
+ 1 nM
+ 3 nM
+ 10 nM
WT ADAMTS13
Relative Proteolytic Activity
Time (min)
E
GoFΔCUB1-2 + CUB1-2
GoFΔCUB1-2
+ 1 nM
+ 3 nM
+ 10 nM
WT ADAMTS13
Relative Proteolytic Activity
Time (min)
C
GoF MDTCS
WT MDTCS
Relative Proteolytic Activity
[CUB1-2] (nM)
F
GoFΔCUB1-2
WTΔCUB1-2
Relative Proteolytic Activity
[CUB1-2] (nM)

**Figure 4**

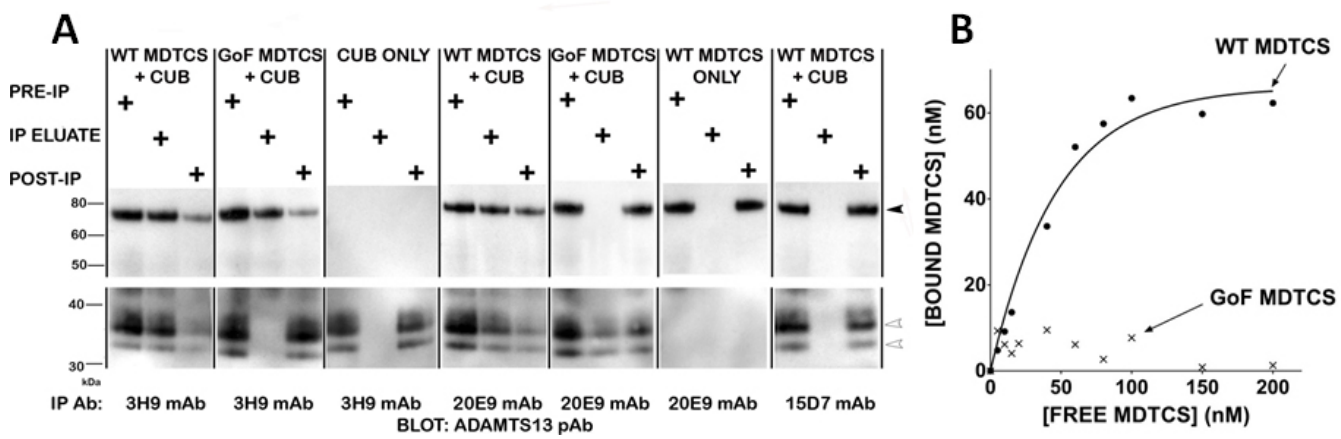


**Figure 5**

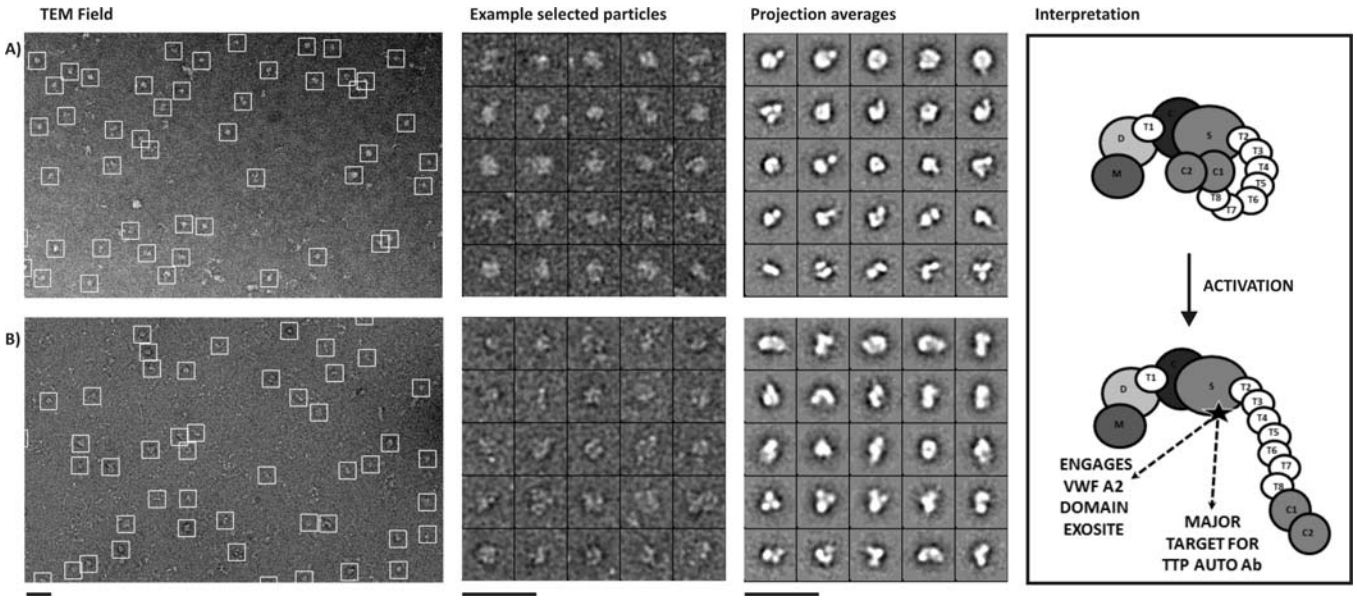

**Figure 6**

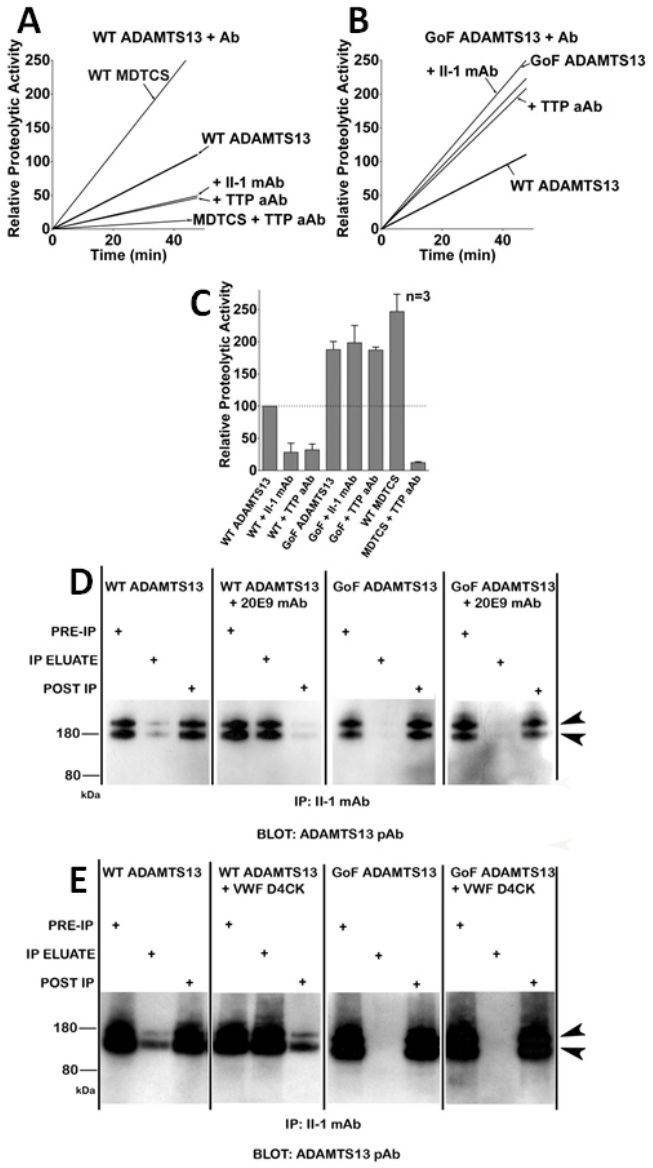
A
WT ADAMTS13 + Ab
WT MDTCS
WT ADAMTS13
+ Il-1 mAb
+ TTP aAb
MDTCS + TTP aAb
Relative Proteolytic Activity
Time (min)
B
GoF ADAMTS13 + Ab
+ Il-1 mAb
GoF ADAMTS13
+ TTP aAb
WT ADAMTS13
Relative Proteolytic Activity
Time (min)
C
n=3
Relative Proteolytic Activity
WT ADAMTS13
WT + Il-1 mAb
WT + TTP aAb
GoF ADAMTS13
GoF + Il-1 mAb
GoF + TTP aAb
WT MDTCS
MDTCS + TTP aAb
D
WT ADAMTS13
WT ADAMTS13 + 20E9 mAb
GoF ADAMTS13
GoF ADAMTS13 + 20E9 mAb
PRE-IP
IP ELUATE
POST IP
180
80
kDa
IP: Il-1 mAb
BLOT: ADAMTS13 pAb
E
WT ADAMTS13
WT ADAMTS13 + VWF D4CK
GoF ADAMTS13
GoF ADAMTS13 + VWF D4CK
PRE-IP
IP ELUATE
POST IP
180
80
kDa
IP: Il-1 mAb
BLOT: ADAMTS13 pAb